Article:

Hutty, T.D., Dong, S. and Brown, S. orcid.org/0000-0001-8229-8004 (2020) Suitability of energy storage with reversible solid oxide cells for microgrid applications. Energy Conversion and Management, 226. 113499. ISSN 0196-8904

https://doi.org/10.1016/j.enconman.2020.113499

Suitability of energy storage with reversible solid oxide cells for microgrid applications

Timothy D Hutty[a], Siyuan Dong[a], Solomon Brown[a]*

[a]*Department of Chemical and Biological Engineering, University of Sheffield, UK*

Abstract

Reversible solid oxide cells (rSOCs) offer the prospect of long term bulk energy storage using hydrogen or methane fuel. Solid oxide technology, whilst less mature than alkaline and PEM technology, offers superior conversion efficiency - especially for electrolysis. Furthermore, the possibility of using the cells reversibly means that separate 'power-to-gas' and 'gas-to-power' components are not needed, potentially reducing costs. In this work, we consider the suitability of energy storage using rSOCs and/or battery storage for a microgrid consisting of houses equipped with solar PV generation. An agent-based simulation model is developed to assess the performance of such a microgrid. The model enables the microgrid's self-sufficiency to be quantified, and hence the possible cost savings through avoided imports of grid power. Sizing of microgrid components is optimised to determine the most cost-effective design capable of achieving given self-sufficiency ratio. Case studies are considered for England and Texas. Initially, designs are considered with hydrogen energy storage only; subsequently, hybrid energy storage is considered, with a community scale battery working alongside the rSOC. Results suggest that payback periods for pure rSOC systems tend to be unfavourable. However, if prices fall to levels foreseen in the literature, a system designed to achieve 50% grid-independence could pay back its investment costs within 20 years. Systems designed for Texas need relatively less storage, owing to the good year-round solar resource; as such, payback time in Texas is superior to the UK. Hybrid storage with battery + rSOC is found to be preferable to battery only systems when (i) high SSR is required and (ii) large over-capacity of PV generation is not possible.

Keywords: energy storage; reversible solid oxide cell; microgrid; hybrid energy storage; self-sufficiency ratio

*Corresponding author.
E-mail address: s.f.brown@sheffield.ac.uk

1. Introduction

1.1 Reversible solid oxide cells (rSOCs) and their applications

In order to mitigate the threat of climate change, it is urgently necessary for energy systems around the world to move away from the carbon intensive fossil fuels upon which they have largely depended in the past. Renewable electricity generation (wind, solar, hydropower, biomass) has the potential to displace generation from fossil fuels. However, wind and solar energy in particular suffer from the problem of intermittency [1]–[3], meaning that the available supply of electricity may not match the demand. Thus energy storage technologies may have an increasing role to play in future energy systems, storing renewable energy when it is available, for consumption when it is required.

Of existing energy storage technologies, most are ill-adapted to store energy for sufficient time periods, or in sufficient bulk, to compensate for fluctuations in renewable output beyond a timescale of hours or days. By contrast, power to gas ('P2G'), the use of electricity to synthesise a gas fuel such as hydrogen or methane, has potential to provide storage of weeks' or months' duration, enabling heavier reliance on renewables by the energy system as a whole. This would typically be accomplished by splitting water with an electrolyser to produce hydrogen gas, which can be stored and subsequently converted back to power using a fuel cell or internal combustion engine. Key difficulties for this form of energy storage are high expense and low round-trip efficiency.

Solid oxide cells (SOCs), although less technologically mature than the more prevalent alkaline or PEM cells, potentially offer superior energy conversion efficiencies both as electrolysers ('P2G') and as fuel cells ('G2P'). SOCs employ ceramic electrolytes and operate at high temperatures (600 – 1000 °C) [4], [5]. These high operational temperatures are associated with some of the key advantages of SOC technology: higher efficiency, tolerance to fuel impurities [4], abundant electrode materials [6], and possibilities for combined heat and power (CHP) applications [7], [8]. At the same time, high operational temperature is also responsible for long start-up times [1], difficulties in pairing with a dynamic load [5], complex and expensive balance-of-plant (BoP) equipment [9], and rapid degradation of cell materials [4]. It is possible for an SOC to operate reversibly, with a single device able to operate alternately as fuel cell and electrolyser [10]; in this case, it is termed a 'reversible solid oxide cell' or rSOC.

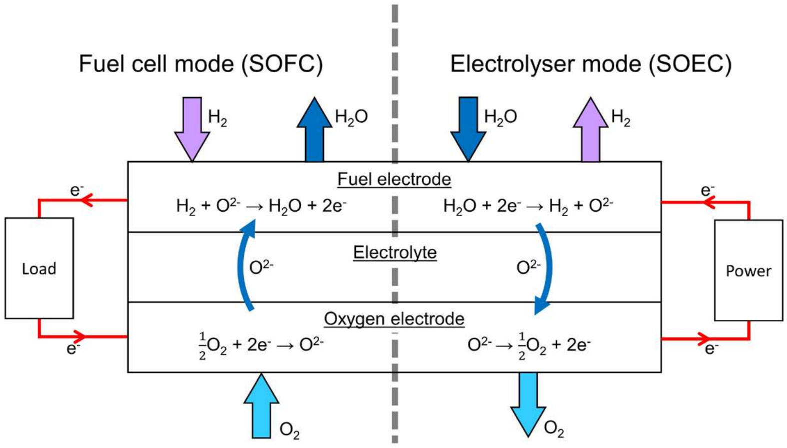

Figure 1. Operation of an rSOC working with hydrogen / steam. Fuel cell mode and electrolyser mode are shown respectively left and right.

The operation of an SOC as both a fuel cell ('SOFC') and electrolyser ('SOEC') is illustrated in Figure 1. The electrolyte of an SOC is usually conductive of negatively charged oxygen ions. In fuel cell mode, the reactions proceed as follows: at the oxygen electrode, oxygen is reduced to O^{2-} and these anions migrate across the electrolyte to the fuel electrode. At the fuel electrode, the fuel is oxidised and combines with O^{2-} to form steam (or CO_2 in the case that the fuel is CO). In electrolysis mode, the reactions are reversed and the ions and electrons flow in the opposite direction. [1].

SOFC is a more mature technology than SOEC, suffering fewer problems with degradation: the Jülich Research Centre reported that their SOFC stack operated for 93,000 hours continuously [11]. Nonetheless, SOEC is attractive because the electrolysis reaction is increasingly endothermic at high temperature [4]. Electrolysis with SOEC is consequently highly efficient, since the reaction recycles unavoidable Joule heat, and may also use external high temperature heat sources. In particular, SOEC is more efficient than PEM or alkaline electrolysers [12]–[14], though degradation represents more of a challenge [1], [4]. There is some evidence though, that reversible use of a cell (i.e. as an rSOC) can actually reverse degradation reactions and prolong the lifetime [15] [16] – but this is still uncertain. Reversible operation can certainly offer a saving in investment costs versus systems with separate devices for P2G and G2P [17]–[19]. An overview of the comparison between SOC with the more mature PEM and alkaline technologies is given in Table 1.

Whilst energy storage using rSOC remains a relatively immature technology, pilot schemes of significant scale have begun to emerge in recent years. The most significant demonstration projects to date have been conducted using SOC technology from German manufacturer Sunfire [20]. The first of these projects was a collaboration between Sunfire and Boeing; this multi-kW scale system, designed with microgrid applications in mind, was commissioned in 2015, undergoing testing at Boeing's Huntingdon Beach facility in southern California. 1920 cells in stacks of 30 could generate 50 kW in fuel cell mode, and absorb 120 kW in electrolyser mode. Hydrogen storage at 250 bar was sized for cycle durations of only 12 hours, although more storage volume could have been added easily and cheaply. The system was online for 1000 hours of testing, undergoing seven full cycles in that time, and achieved electrolysis efficiency of ca. $60\%_{LHV}$ (allowing for steam generation and hydrogen compression). In comparison, fuel cell mode was found to be $49\%_{LHV}$ efficient, resulting in a round-trip efficiency of around 30%. Whether any degradation was observed over the test's duration is not reported.

Another trial using Sunfire rSOC technology is reported in [21]–[24]; this is the 'GrInHy' or 'Green Industrial Hydrogen' project. The 143 kW rSOC was installed at a steelworks, where the ready availability of waste heat enabled the energy cost of steam generation to be avoided. Furthermore, generated hydrogen could be used by the steelworks as a reducing agent (in place of coke) and for annealing. Thanks to the use of waste heat, electrical round-trip efficiency was able to approach 40%. The rSOC demonstrated a good level of flexibility, with transition between hot standby and 100% load taking respectively 24 and 20 minutes for electrolysis and fuel cell operation;

partial load operation down to respectively 50% and 40% was possible with no efficiency penalty. Voltage degradation of 0.8% per thousand hours was observed in electrolysis mode. In practice, it was more economically viable to use generated hydrogen in the steelworks, and run fuel cell mode using CH_4, rather than using the rSOC as a true energy store.

Table 1. Comparison of electrolytes: solid oxide versus alkaline and PEM.

Electrolyte	Alkaline	PEM	Solid oxide
Operating temp. (°C)	<100 °C [4], [5]	< 140 °C [1], [5]	600 – 1000 °C [4], [5]
Electrolysis efficiency (system level)	43 - 67% [12]–[14]	40 - 67% [12]–[14]	63 - 82% [12]–[14]
Fuel cell efficiency (system level)	45 – 60% [25]	45 – 50% [25]	35 – 61% [14], [21], [25], [26]
Startup time	15 minutes [5]	< 15 minutes [5]	From cold: hours [1], [5] From hot standby: minutes [22], [27]
Dynamics and flexibility	Min partial load 10-40% [12]	Suitable for partial load and variable load operation [5], [12], [28]–[30]	Rapid load changes can cause problems due to thermal stress [1], [5].
Key advantages	**Most mature technology for electrolysis; reliable, safe, long lifetime** [4], [5], [31].	**Preferred for fuel cell applications** [32]; electrolyser yields highest purity hydrogen [4].	Use waste heat to boost electrolysis efficiency [5]; work with carbonaceous species; possible CHP applications; possible reversible operation.
Key challenges	Inferior dynamic response to PEM; corrosive electrolyte [5].	Expensive membranes, catalyst materials [4] [5]; less scalable than alkaline technology [4].	Immature technology [4] [5]; rapid degradation especially for SOEC [4] [33]; thermal management is challenging [5].
System cost for electrolysis	**lowest** 700 – 1500 € / kW [12], [13], [33], [34]	**medium** 800 – 2300 € / kW [12], [13], [33], [34]	**highest** >2000 € / kW [12] [33] **Potential for cost reduction**, possibly to 760 € / kW [33]

A third notable pilot project is REFLEX [27], [35], [36], a European project coordinated by CEA-Liten, using rSOCs manufactured by Estonian company Elcogen. The project is currently in development, with a 'Smart Energy Hub' to be built at Envipark, Turin, Italy. This will incorporate three rSOC modules for total electrolysis capacity of 120 kW, with storage of CHG at 200 bar, and Li-ion batteries providing shorter term storage. The Smart Energy Hub will be co-located with solar and hydro generation and will supply both heat and power. The stated objective is to achieve $90\%_{LHV}$ efficiency for electrolysis, and $50\%_{LHV}$ for fuel cell operation. Testing of the facility is to take place in 2020.

With sophisticated balance-of-plant (BoP) configurations, it may be possible to improve on the efficiencies observed in these real-world trials - and a great deal of work has been done to model rSOC energy storage at the BoP scale. The thermal management of the plant is key to unlocking higher RT efficiency. Many proposed plants use thermal energy storage (TES) to enable surplus heat from fuel cell mode to supply heat for electrolysis; waste heat from the compression of hydrogen or other heat sources may also be used. For instance, modelling by Giap et al [37] found that the use of industrial waste heat in an rSOC plant could enable RT electrical efficiency to reach 53.8%; the researchers felt this to be too low, recommending the use of TES to boost efficiency further. Ren et al [38] modelled a concept for rSOC energy storage in which fuel and exhaust species would remain always in a pressurised vessel, with bronze used as a phase change material for TES. The system, for which the suggested storage duration was 'short time periods, such as hours', was modelled to achieve round-trip efficiency up to 64%. Perna et al [39] modelled a 100 – 200 kW rSOC energy storage system, wherein coupling of heat sources and sinks, together with the use of diathermic oil for TES, enabled the modelled RT efficiency to reach 60%. The proposed plant would also supply hot water, with cogeneration efficiency of 91%. Lototskyy et al [8] present a novel rSOC system designed for combined cooling, heating and power; various metal hydride beds would be used to store both hydrogen and heat. Their modelling suggested that the system, which was proposed for use with domestic solar PV, could achieve electrical RT efficiency of 46.7%, and tri-generation efficiency of 70.6%. Akikur et al [40] propose a solar + rSOC plant for CHP. Solar PV would provide power for electrolysis, with concentrated solar power providing heat for steam generation. Mathematical modelling suggested electrical round-trip efficiency of around 38%. Economic analysis found that the cost of electricity for the plant would be $0.0676 / kWh, although the cost of the hydrogen storage component was neglected.

Ullvius and Rokni [41] suggest a rather different approach to extracting additional value from an rSOC plant: the use of waste heat for water desalination using direct contact membrane distillation. Such a system was modelled for deployment on the South African coast, with concentrated solar power providing both heat and power for electrolysis. The plant would export 500 kW of power continually, and also generate 8.5 tonnes of fresh water per day.

Giorgio and Desideri have proposed an rSOC system using TES in close contact with the stack [42]. This would be either sensible heat storage using a ceramic material or latent storage using a eutectic metal alloy. Hydrogen would be stored at 108 bar. In similar fashion to [43], two configurations were considered: one in which water vapour would be condensed out of the off-gas, and one in which the vapour would be stored (removing the need for a steam generator). In the first configuration, surplus heat during SOFC mode was transferred to a steam drum in preparation for SOEC mode. This configuration was found to be capable of 72% RT efficiency, with either form of TES. However, electrolysis could not continue for long before external heat was needed for steam generation. The stored vapour configuration could achieve RT efficiency of only 64% - although this would reach 74% if the stack could be pressurised. The evaluation cycles considered in this research were of short duration, with two hours of fuel cell mode followed by electrolysis.

1.2 Hydrogen energy storage for microgrids – existing work

There is a fair amount (e.g. refs [44]–[51]) of extant research on the applications of hydrogen energy storage for distributed scale, microgrid type applications. Such research often includes optimisation of technology choice, sizing, or dispatch over time, and some assessment of the economic case for the storage. Common themes include concerns with high costs; the desirability of hybridisation with shorter term storage; and the extraction of additional value through niche applications such as hydrogen powered vehicles. These studies overwhelmingly consider PEM or alkaline technology, and studies assessing applications of rSOCs are much less numerous. However, Baldinelli et al [52] propose a concept in which rSOCs are hybridised with flywheel energy storage to smooth out short term load fluctuations. A control algorithm is proposed to determine charge / discharge of the two energy stores, and the system's components are sized for a microgrid consisting of a number of homes with PV generation. The hybrid system was able to moderately increase the microgrid's self-sufficiency (from 52.1% to 58.0%); economic analysis was not conducted. Sorrentino et al [53] present a microgrid consisting of an rSOC and hydrogen storage, as well as PV and a vertical axis wind turbine, for the supply of power to an apartment complex. The use of additional short-term storage was recommended but not modelled. Sizing of the microgrid's components was optimised to achieve the lowest possible payback time; the optimal system would store 144 kg (~5 MWh) of hydrogen gas, enabling up to 10 days of grid independence, and was claimed to achieve payback in just over 11 years. However, CAPEX estimates appear to have been rather optimistic (rSOC $400 / kW; PV €817 / kW).

1.3 Novel contribution of this work

Whilst simulations at BoP level are abundant in the literature, studies on actual applications for rSOC energy storage are few. Literature on microgrid applications for hydrogen energy storage typically assumes use of PEM or alkaline technology with separate components for gas-to-power and power-to-gas. Here we consider the design of a microgrid using rSOC specifically. Accordingly, key characteristics of rSOCs (limited partial load capability; limited ramp rate; coupled fuel cell and electrolysis capacity) are included in the model. Whilst there is some extant work on rSOC based microgrids, it gives an incomplete picture, especially on economic aspects. Here we attempt to give a fuller picture, through inclusion of different scenarios for location, cost and performance of the technology. We also obtain some indication of the circumstances under which rSOC can compete with, or complement, battery storage.

The rest of the paper is structured as follows: in Section 2, the simulation model constructed in AnyLogic is described, including its various sub-models. Section 3 introduced the case studies and presents the results obtained from them; conclusions are summarised in section 4.

2. Model construction

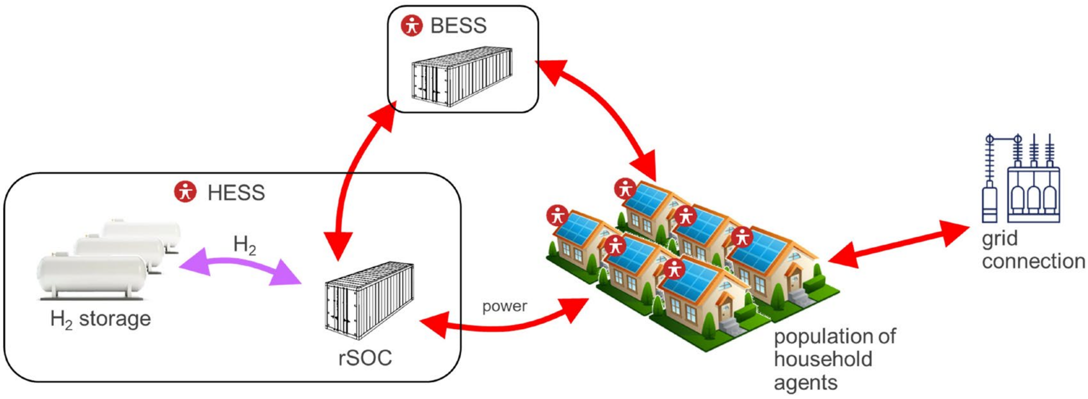

Figure 2. Schematic representation of the microgrid model. Most elements of the model are represented as agents (denoted by the red icons).

2.1 Overview

The purpose of this work is to simulate how an rSOC energy storage system might perform in a real-world distributed energy context. To this end, a simulation has been constructed of a small distributed energy system (or microgrid), consisting of a residential area with local renewable generation, supported by a hydrogen energy storage system (HESS) using rSOC, and a grid connection. A community battery, which can be used in tandem with the rSOC, is also modelled. A schematic of the simulation is provided in Figure 2. This simulation has been implemented using the multi-paradigm simulation programme AnyLogic [54]. Agent-based modelling provides versatility in modelling the components of the microgrid as distinct entities, and readily allows for combination of social or economic models with technical ones. Most elements of the microgrid model are agents (or sub-agents), including individual households – although the behaviour of households on an individual level is not discussed here.

We now present the various sub-models in more detail.

2.2 rSOC model

For the present work a detailed BoP model is not desirable. Instead, the rSOC is described by a few key parameters (see Table 2): the nominal capacity of the rSOC in each mode; the partial load range; the efficiency and the achievable ramp rate. The efficiency values are intended to incorporate all BoP losses, including power electronic converters and (for electrolysis mode) steam generation.

Table 2. Parameters used to characterise the rSOC system.

Parameter	Symbol	Unit	**Values from** [10], [21]
Electrolyser mode nominal capacity	P_{SOEC}	kW_{AC}	166
Electrolysis efficiency*	η_{SOEC}	MJ / kg_{H2}	172.5
Electrolyser partial load range	-	%	50 … 125%
Fuel cell mode nominal capacity	P_{SOFC}	kW_{AC}	30
Fuel cell nominal efficiency*	η_{SOFC}	MJ / kg_{H2}	60
Fuel cell partial load range	-	%	30 … 100%
Ramp rate	Δ	% of nominal capacity per minute	5%

*including steam production and all BoP other than H_2 compression

The state of the rSOC at a given point in time is described by the partial load percentage, which here we shall represent by μ. This can range from -100% (or below) for electrolysis to +100% for fuel cell mode, where +/-100% are respectively mapped to the nominal loads P_{SOFC} and P_{SOEC} for fuel cell and electrolyser mode. Thus, the AC power either generated (+) or consumed (-) is given by:

$$P_{AC} = \begin{cases} \frac{\mu}{100} \times P_{SOFC}, \mu \geq 0 \\ \frac{\mu}{100} \times P_{SOEC}, \mu < 0 \end{cases} \quad [1]$$

The consumption or production of hydrogen, $\dot{m}_{H2}$ in kg per hour is then given as follows:

$$\dot{m}_{H2} = \begin{cases} \frac{3.6 \times P_{AC}}{\eta_{SOFC}}, & \mu \geq 0 \\ \frac{3.6 \times P_{AC}}{\eta_{SOEC}}, & \mu < 0 \end{cases} \quad [2]$$

The rate at which μ can change is limited by the ramprate Δ. Work from GrInHy [22], [24] suggested that their electrolyser could ramp its output by least 10 kW/min, which was about 7% of the nominal 142.9 kW load. Here Δ defaults to a conservative value of 5% of nominal load per minute. When changing mode, the rSOC can pass through 'forbidden' load points that are outside the permissible partial load range; however, it is not permitted to remain continually at such load points. It is worth noting that although we allow load to vary continuously in the permitted range, it is also possible that a real system might only have discrete partial load settings.

As a starting point, the rSOC model is parametrised based on the data available from the various trials of Sunfire's rSOC technology [10], [21]. P_{SOEC} and P_{SOFC} may be scaled up or down, but will be assumed to remain in proportion. With efficiencies of 172.5 MJ/kg_{H2} for electrolysis, and 60 MJ/kg_{H2} for fuel cell mode, round-trip efficiency is just under 35%, before allowing for the electrical work to compress the hydrogen for storage.

2.3 Hydrogen storage model

During electrolysis mode, additional power is required for compression of hydrogen; this is calculated as follows. The isentropic compression energy W for compression of 1 kg of hydrogen between pressures P_1 and P_2 is given in kJ by [55]:

$$W = \frac{\gamma RT}{\gamma - 1}\left(\left(\frac{P_2}{P_1}\right)^{\frac{\gamma-1}{\gamma}} - 1\right) \cdot {M_{H2}}^{-1} \quad [3]$$

where T is temperature in Kelvin, R is the ideal gas constant; γ = 1.41 is hydrogen's heat capacity ratio and M_{H2} = 2.014 g / mol is hydrogen's molar mass. Multi-stage compression with intercooling can allow the required work to be less than the isentropic work. Whilst the specific configuration of compressors and intercoolers is outside the scope of this work, we assume that the hydrogen storage system would be designed with intercooling. Accordingly, we assume that the work of compression can be reduced to 74.5% of the isentropic work, where this proportion is derived from reference [55]. Thus, the mass flow rate of hydrogen $\dot{m}_{H2}$ in kg/hour can be used to find the electrical load P_{comp} for the compression of hydrogen (in kilowatts):

$$P_{comp} = \frac{0.745 \cdot W \cdot \dot{m}_{H2}}{3600} \quad [4]$$

This power is drawn from the microgrid in addition to the power required by the rSOC itself.

2.4 Battery model

Table 3. Parameters used to characterise the community battery.

Parameter	Symbol	Unit	Default value
Nominal capacity	C_{BESS}	kWh	-
DC to DC efficiency	η_{BESS}	-	0.94 [56]
Inverter efficiency	η_{DCAC}	-	0.95 [22]
Rectifier efficiency	η_{ACDC}	-	0.95 [22]
C rate	R_{BESS}	h^{-1}	2 [57]
Self-discharge rate	Λ	h^{-1}	4.2×10^{-5} [58], [59]
State of charge range	-	%	5 – 95%

The community scale battery energy storage system (BESS) is modelled primarily in terms of its capacity in kWh (C_{BESS}), its achievable C rate (R_{BESS}) and its DC to DC round-trip efficiency η_{BESS}. Unlike for the rSOC, the efficiencies of the power electronic converters are accounted for separately as η_{DCAC} and η_{ACDC}, both equal to 0.95 [22]. Self-discharge is also included, although impact of this is expected to be negligible, with the default value of 4.2×10^{-5} h^{-1} equating to 3% per month. Here the model is parametrised to represent Li-ion battery technology, based on figures from [56], [57].

For simplicity, the losses according to η_{BESS} are modelled as though they occur entirely during the charging of the battery. R_{BESS} is interpreted such that R_{BESS}^{-1} gives the minimum time in hours to either fully charge or discharge the battery. In contrast with the rSOC, there is no lower limit set on the charge / discharge power: i.e. partial load can be varied all the way down to 0%. Similarly, there is no restriction placed on the battery's ramp rate. It is reported in [57] that a 2 MW battery is able to fully reverse its output in 40 milliseconds; this is many orders of magnitude smaller than the time resolution considered here.

Where P_{ch} is the AC power supplied to the battery, P_{dch} is the AC powered discharged from the battery, and E_{BESS} is the electrical energy stored in the battery, the model imposes the following equations (with hours as time unit):

$$\dot{E}_{BESS} = \eta_{BESS} \cdot \eta_{ACDC} \cdot P_{ch} - \frac{P_{dch}}{\eta_{DCAC}} - \Lambda \cdot E_{BESS} \quad [5]$$

$$0 \leq E_{BESS} \leq C_{BESS} \quad [6]$$

$$0 \leq P_{ch} \leq \frac{R_{BESS} \cdot C_{BESS}}{\eta_{BESS} \cdot \eta_{ACDC}} \quad [7]$$

$$0 \leq P_{dch} \leq \eta_{DCAC} \cdot R_{BESS} \cdot C_{BESS} \quad [8]$$

Equation [5] is modelled using system dynamics, with E_{BESS} represented as a stock, and flows of power in or out according to the charge, discharge and self-discharge terms. A statechart is used to classify the battery as 'empty' once $E_{BESS} \leq 0.05 \cdot C_{BESS}$, 'full' when $E_{BESS} \geq 0.95 \cdot C_{BESS}$, and 'partially charged' otherwise.

2.5 PV model

Solar generation profiles are simulated using measured hourly data for global horizontal irradiance (GHI). The model outlined here uses GHI to predict the output of PV panels with arbitrary tilt and orientation. Clearness index k_t is calculated as [60]:

$$k_t = \frac{GHI}{I_{ET} \sin \alpha_s} \quad [9]$$

where α_s is the sun's altitude above the horizon, and I_{ET} is the normal irradiance above the Earth's atmosphere, which averages 1367 Wm^{-2}, varying by ±3.3% throughout the year. Erbs' model [61] is then employed to predict diffuse fraction k_d from the value of k_t, so that the diffuse horizontal irradiance (DHI) is known. The simplifying assumption is made that diffuse irradiance is distributed evenly across the sky. The total radiation I_{pv} incident on one square metre of tilted panel can now be calculated [62]:

$$I_{pv} = direct\ contribution + diffuse\ contribution + reflected\ contribution$$

$$= \frac{GHI(1-k_d)}{\sin\alpha_s}\cos\theta_i + GHI \cdot k_d \cdot \frac{1+cos(\zeta_{pv})}{2} + GHI \cdot R_{gr} \cdot \frac{1-cos(\zeta_{pv})}{2} \qquad [10]$$

Here, θ_i is the incident angle between the sun's rays and the normal to the tilted PV panel, and R_{gr} is the reflectance of the ground, taken to be 0.2. θ_i is obtained from the sun's azimuth φ_s and altitude α_s, and the panel's azimuth φ_{pv} and tilt ζ_{pv}, as follows [62]:

$$cos(\theta) = sin(\zeta_{pv})cos(\varphi_{pv})cos(\alpha_s)cos(\varphi_s) + sin(\zeta_{pv})sin(\varphi_{pv})cos(\alpha_s)sin(\varphi_s) + cos(\zeta_{pv})sin(\alpha_s) \qquad [11]$$

Assuming a fixed efficiency η_{pv} and area A for the PV installation, the generated power P is simply

$$P = \eta \cdot A \cdot I_{pv} \qquad [12]$$

5.75 m^2 of PV is assumed to correspond to 1 kW_p capacity [63]. Validation of the PV model was conducted using hourly irradiance data for 2015 recorded at Rothamsted [64], and corresponding PV generation data for a 3.96 kW installation located 5.9 km to the south-west [65]. Modelled and measured generation were compared at daily resolution over the year, and at hourly resolution over a two-week period in June. At daily resolution, the model achieved mean absolute error of 0.769 kWh / day (7.6% of average daily generation). At hourly resolution, mean absolute error was 0.112 kWh/h. The errors observed were checked for correlation with temperature (hourly average; daily min, max and average) and irradiance. No significant correlations were found, suggesting that a simple model with constant efficiency is adequate for the UK climate.

For the results presented below, the model was calibrated by enforcing a capacity factor of 11.8% for a south-facing panel at 40° tilt angle in SE England [66]; this was achieved by setting $\eta_{pv} = 0.1541$. For the SE England case study, houses are assumed to have random orientation, resulting in diversity between the different rooftop PV installations; the *average* capacity factor then becomes ~11.0%.

2.6 Control strategies

2.6.1 Control of rSOC without BESS

Since time-variable import / export tariffs are not considered in this work, the most cost-effective dispatch of a single energy storage type, whether battery or rSOC, is trivially achieved via a greedy algorithm. At every time step, the energy surplus (or deficit) is calculated, and the energy storage will absorb (or supply) as much of this as possible, as constrained by its capacity, partial load capability, and state of charge.

2.6.2 Control of hybrid energy storage

When rSOC and BESS are both used, the control is less trivial, even in the absence of variable tariffs. A naïve approach is to continue to use a greedy algorithm, which preferentially uses the battery because of its superior efficiency. For instance, all surplus generation would be sent to the battery until the battery is full, after which the rSOC would take over. This is an unsatisfactory approach; the two energy stores need to be worked simultaneously, otherwise the rSOC capacity would have be sized larger to absorb the largest deficits / surpluses by itself.

In this work, the approach taken is to plan the rSOC dispatch in advance, whilst the BESS continues to follow a 'greedy' approach, compensating for the remaining surplus/deficit. Five-day forecasts, at one-hour resolution, are made for electrical load and generation, and passed to a controller agent. Forecasts for load and irradiance assume perfect foreknowledge; PV generation forecast is calculated from irradiance by modelling the many separate solar rooftop installations as just three large arrays at different orientations.

The controller works by setting bounds $(P_{max,d})_{1\le d\le 5}$ and $(P_{min,d})_{1\le d\le 5}$ on the net load absorbed by the rSOC on each day d of the forecast. For each time step, the rSOC responds to the microgrid's net load as far as possible (see Figure 3), as constrained by $P_{min,d}$ and $P_{max,d}$, as well as its partial load capability and the H_2 storage capacity. Remaining load imbalances are then addressed by the battery and the grid connection, in that order. In this way, an hourly schedule $\left(P_{HESS,t}\right)_{0\leq t<120}$ for the rSOC net load is produced. The full details of this method are given in the appendix.

Thus, there are ten decision variables for the controller to optimise, $\left(P_{max,d}\right)_{1\leq d\leq 5}$ and $\left(P_{min,d}\right)_{1\leq d\leq 5}$. The objective function is defined as the (negative) value of effective energy stored at the end of the forecast period, plus the cost of imported power during the forecast period, as follows:

$$-c_{store}\cdot\left(\frac{\eta_{SOFC}}{3.6}\cdot m_{H2,120}+\eta_{DCAC}\cdot E_{BESS,120}\right)+c_{grid}\cdot\sum_{t=0}^{119}P_{imp,t} \qquad [13]$$

Here, $E_{BESS,120}$ is the final kWh stored in the battery; c_{grid} is the cost of grid-imported power, and c_{store} is the value assigned to energy stored at the end of the forecast period. c_{store} is set to £0.10 for the case study in this work. $c_{store} < c_{grid}$ is essential or the rSOC will never use fuel cell mode.

The controller carries out this optimisation using the OptQuest optimisation engine [67]. OptQuest is well suited to problems with low dimensionality and unknown structure, which is why the controller has been designed in this manner. The controller runs at 6pm every day to update the schedule for the rSOC.

Figures 4 and 5 show microgrid dispatch over the same three days for microgrids with differently sized energy storage components. Note that the controller produces markedly different schedules in each case. In Figure 4, the rSOC is small but the battery large. The controller sets the maximum load negative, close to the minimum (similar to Figure 3b), so that electrolysis continues steadily through the night, powered by the battery. The battery manages the day/night cycling, whilst the stored hydrogen climbs continually. In Figure 5, the battery is not large enough for this approach. The maximum load is set positive, so that fuel cell mode is active during the night (similar to left hand side of Figure 3). The rSOC and battery both contribute to the day/night cycling.

For the microgrid specification in Figure 4, the control method described here reduces annual grid imports by around 15% compared to a greedy algorithm.

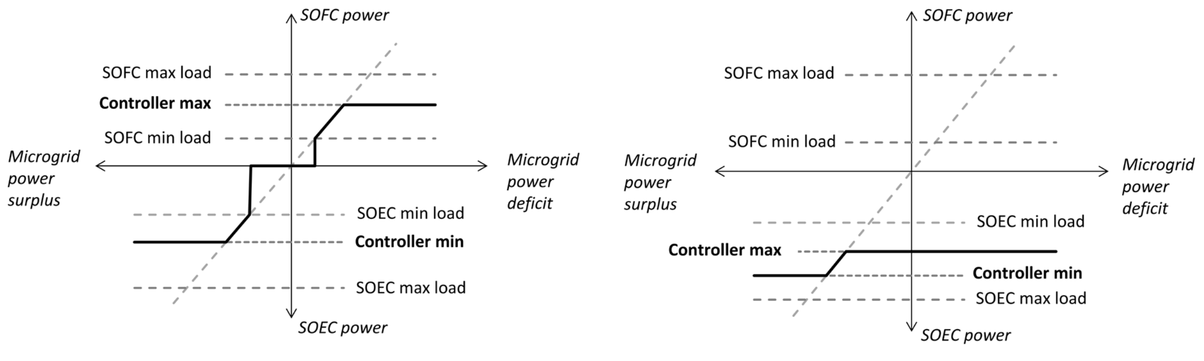

(a) (b)

Figure 3. Illustrates how the response of the rSOC to the microgrid's deficit / surplus is curtailed by the maximum and minimum daily load imposed by the controller. The rSOC may be permitted to operate in both modes, as in (a), or constrained to operate in only one mode – as in (b), where electrolysis carries on even when the microgrid is in deficit. Operation in one mode throughout the day is likely to occur when battery capacity is large but rSOC capacity is small.

(a)

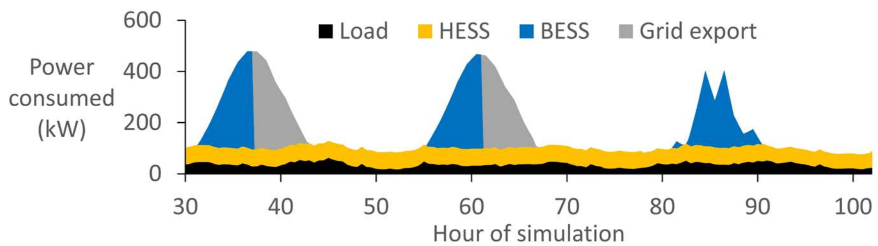

(b)

(c)

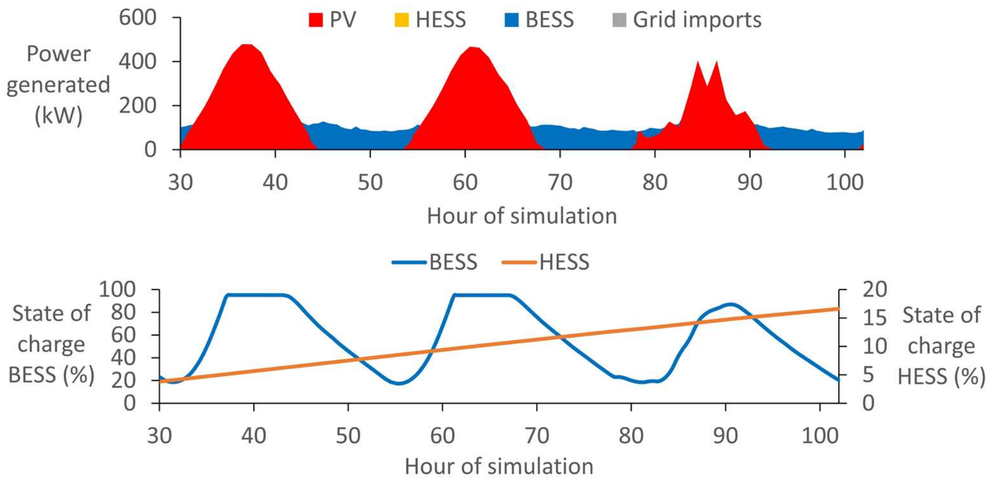

Figure 4. Example dispatch of the microgrid with hybrid energy storage over three days in early May. 6 kW PV per dwelling; 50 kW rSOC; 1438 kWh battery.
(a): power consumed; (b) power generated; (c) state of charge of each energy storage.

(a)

(b)

(c)

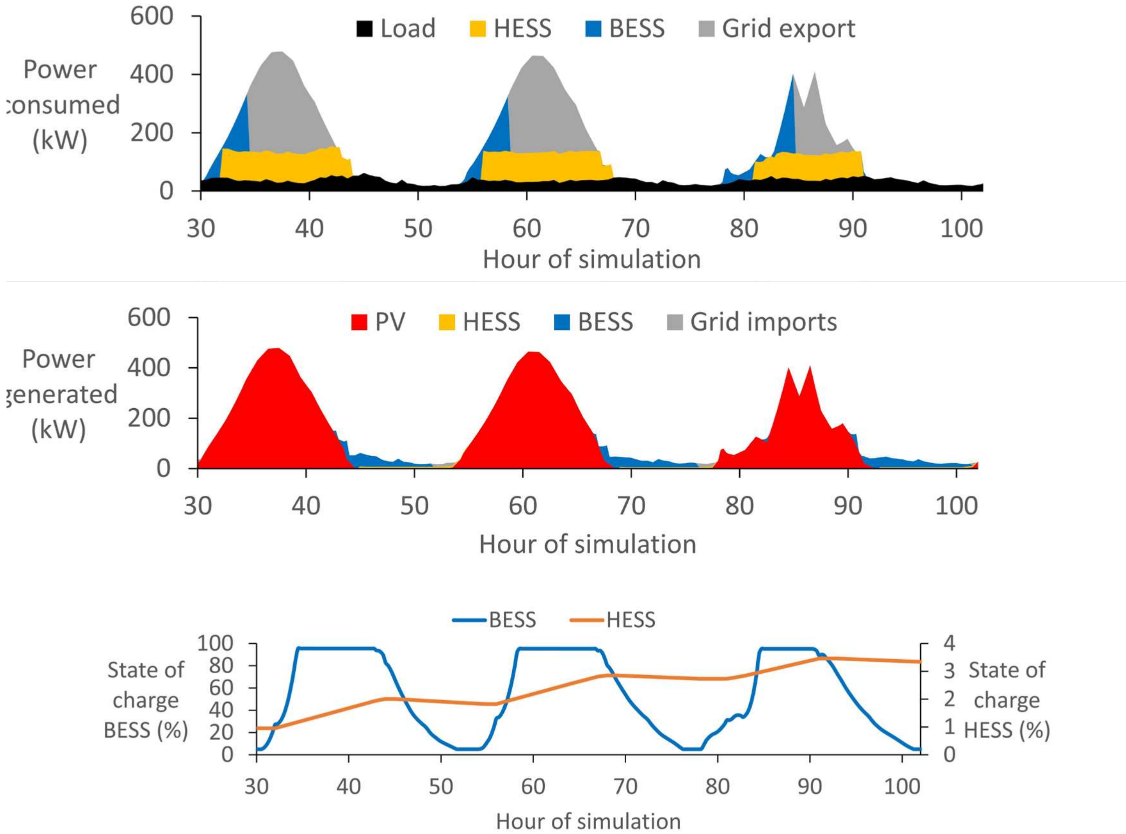

Figure 5. Example dispatch of the microgrid with hybrid energy storage over three days in early May. 6 kW PV per dwelling; 75 kW rSOC; 300 kWh battery.
(a): power consumed; (b) power generated; (c) state of charge of each energy storage.

2.7 Performance metrics; scenarios for cost and efficiency; optimisation of technology choice and sizing

Table 4. Estimates for installed CAPEX (two cost scenarios)

Technology	Symbol	Cost scenario 1 (Baseline estimate)	Cost scenario 2 (Low/future estimate)	References
rSOC	c_{rsoc}	£2000 / kW_{SOEC}	£750 / kW_{SOEC}	[12], [33]
PV	c_{pv}	£1750 / kW_p	£1000 / kW_p	[68]
H_2 storage	c_{H2}	£1000 / kg (£30 / kWh)	£333 / kg (£10 / kWh)	[10], [69], [70]
Li-ion battery storage	c_{BESS}	£500 / kWh	£500 / kWh	[71], [72]

Self-sufficiency ratio (SSR) for the community is defined to be the annual energy consumed which is *not* imported from the grid, as a proportion of total energy consumption:

$$SSR = \frac{(energy\ consumption) - (grid\ imports)}{(energy\ consumption)} \quad [14]$$

As well as quantifying the microgrid's grid-independence, SSR gives a basic measure of environmental benefit; under the simplifying assumption that grid emissions are constant, SSR is equal to the reduction in emissions per unit of electricity consumed by the microgrid. In fact, SSR may give an underestimate of emissions curtailment, since the HESS and BESS are most likely to discharge in the early evening, when grid emissions are often above average. To give a rough idea for the cost of the energy system, based on the installed capacities of PV, rSOC and hydrogen storage, estimates for these technologies' installed CAPEX costs are used as shown in Table 4. Initial work uses the higher 'baseline' figures; we then consider a more optimistic future scenario (although the installed cost of battery storage is the same for both). Accordingly, the installed cost for the microgrid is estimated as:

$$c_{total} = c_{pv} \cdot n \cdot C_{pv} + a_{HESS} \cdot \left(c_{rsoc} \cdot P_{SOEC} + c_{H2} \cdot m_{full} \right) + a_{BESS} \cdot c_{BESS} \cdot C_{BESS} \quad [15]$$

Here, n represents the number of houses; C_{pv} the mean kW of installed PV per house; and m_{full} the capacity of the hydrogen storage in kg. a_{HESS} and a_{BESS} are binaries expressing whether each form of storage is installed.

Annual savings achieved by the microgrid are considered equal to the avoided cost of grid-imported power. The retail price of electricity c_{grid} is estimated to be £0.144 / kWh for the SE England study, and \$0.127 / kWh for Texas. Simple payback periods are then calculated simply as CAPEX divided by annual savings:

$$payback\ period = \frac{c_{total}}{c_{grid} \cdot SSR \cdot E_{year}} \quad [16]$$

where E_{year} is the microgrid's annual electricity consumption in kWh, and c_{grid} is the cost of imported power per kWh.

For comparison between the case studies, an approximate exchange rate of \$1.25 to £1 is assumed. Two scenarios are considered for the efficiency of rSOC technology. The first (baseline) scenario is based on technology already demonstrated at scale by Sunfire [10], [21], achieving round-trip efficiency just under 35%. The second scenario assumes round-trip efficiency of 60%. Balance-of-plant level simulation work seen in the literature suggests that this may be realistic for rSOC technology in the future.

Table 5. Scenarios for efficiency of rSOC technology.

	Efficiency scenario 1 (Baseline estimate)	Efficiency scenario 2 (High/future estimate)
η_{SOEC}	172.5 MJ/kg_{H2}	120 MJ/kg_{H2}
η_{SOFC}	60 MJ/kg_{H2}	72 MJ/kg_{H2}

rSOC round-trip	34.8%	60%

All optimisations are conducted using the OptQuest global optimisation engine [67], [73]. In this work, optimisation of microgrid design has the minimisation of payback period (see Equation 16) as the objective, subject to constraints on the SSR to be achieved. Decision variables are summarised in Table 6.

Table 6. Decision variables for the optimisation of the microgrid design.

Variable	Type	Description
a_{HESS}	Binary	Installation of HESS
a_{BESS}	Binary	Installation of BESS
C_{pv}	Continuous	Capacity of PV (kW_p per house)
P_{SOEC}	Continuous	Capacity of rSOC (kW)
m_{full}	Continuous	Capacity of H_2 storage (kg)
C_{BESS}	Continuous	Capacity of BESS (kWh)

3. Results

This section falls into the following parts. Firstly, the two case studies are introduced. Secondly, rSOC energy storage is considered for both of these, with optimisation of microgrid design under different scenarios. Thirdly, hybrid energy storage with battery and rSOC is considered (for the England case study only).

3.1 Case Studies

The model described above has been employed for two case studies. In both cases the scenario is a small residential community, each house equipped with rooftop PV, with the rSOC energy storage serving the whole community. The location for case study 1 is the south-east of England. Electrical load data comes from a smart-meter trial in London carried out by UK Power Networks and has half-hourly resolution [74]. Climate data was recorded by the UK Environmental Change Network at Rothamsted (near London) and has hourly resolution [28]. Rooftop PV installations are assumed to average 3 kW_p [75]. Simulations begin on May 1st, around the time of year that daily surpluses of solar power begin.

The second case study is located in Austin, Texas, USA. Two factors motivate this choice. Firstly, Pecan Street Inc. have a rich set of freely available data for many houses in Austin, with measured time series data for both electrical load and PV generation [76]. Secondly, the location provides a good contrast to the UK case study: peak electricity demand is in summer (owing to air-conditioning loads) rather than winter; PV installations tend to be larger and have higher capacity factor, and overall domestic electricity consumption is also much higher. These differences may be seen in Figure 6 and Table 7. Simulations for this case study begin with the calendar year, since solar surplus is experienced in late winter and early spring.

Table 7. Details of the two case studies. All parameters are for the microgrid as an aggregate whole.

	SE England	Austin, Texas
No. of dwellings	92	92
Annual electricity consumption	384 MWh	1090 MWh
PV installed	276 kW_p	508 kW_p
Annual PV generation	267 MWh	633 MWh
Capacity factor	11.0%	14.2%
SSR	33.4%	36.1%
Annual cost of imported power	£36830	$88494

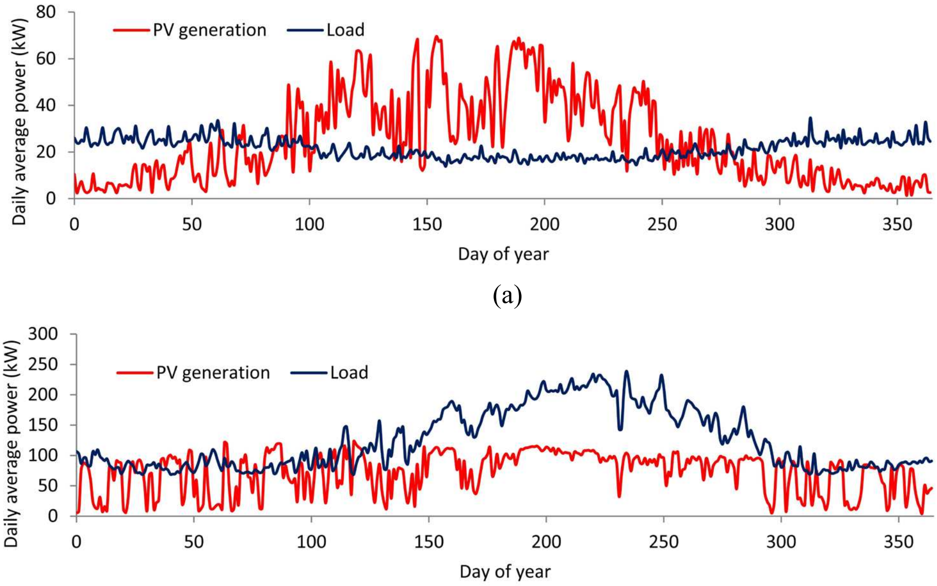

(a)

(b)

Figure 6. Average daily load and PV generation for the community of 92 dwellings, for (a) SE England and (b) Austin, Texas, over one year, prior to deployment of any energy storage. Clear differences between the case studies are evident. Electrical load is higher throughout the year in the Austin study, and peaks dramatically during the summer, rather than the winter. PV output is also more constant over the course of a year (due to both climate and latitude, it is assumed). PV output is modelled for England case study, but comes from Pecan Street Inc. data for Texas.

3.2 Initial results with existing PV capacity

Firstly, we explored what the rSOC energy storage could achieve alongside the baseline amount of installed PV. To determine the maximum possible impact, the rSOC capacity P_{SOEC} was optimised to achieve maximum SSR (with H_2 storage volume unlimited and PV capacity fixed). Correct sizing of the rSOC is important, since its partial load capability is limited [10], [21], [77]. Table 8 gives a summary of the results for each case study. For both locations, the rSOC + H_2 storage system would enable SSR to increase to about 42% (up from 33% and 36% for the UK and Texas respectively). This is the maximum SSR achievable without installing additional PV capacity.

The storage profile over the year (in terms of mass of stored H_2) is shown in Figure 7, for each location. For the Texas case study, only short term cycles of at most a week's duration are observed. This is unsurprising, since a daily surplus of solar energy is rare (see Figure 6) and it tends to suggest that long term storage using hydrogen is hard to justify here, without an increase in PV capacity. For the UK study, surpluses of solar power are common enough in the summer that the storage profile does display a long-duration cycle.

The increase in SSR achieved by the storage results in lower payments for imported grid power. When comparing to the microgrid equipped with PV only, the rSOC + H_2 storage saves around £5000 p.a. in the UK, or \$8000 p.a. in Texas. These savings are far from sufficient to offset the extra investment; in both locations, payback periods for the addition of storage exceed 60 years – far beyond the system lifetime. The addition of the HESS energy storage is thus hard to justify here, with poor economics and only a small increase in SSR to improve environmental performance.

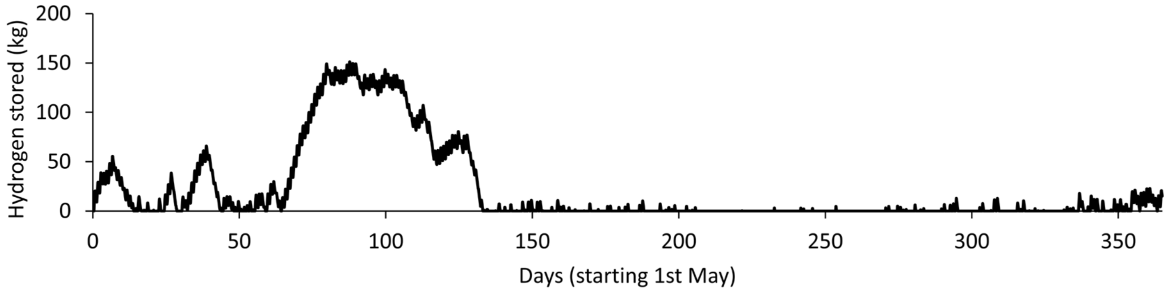

(a)

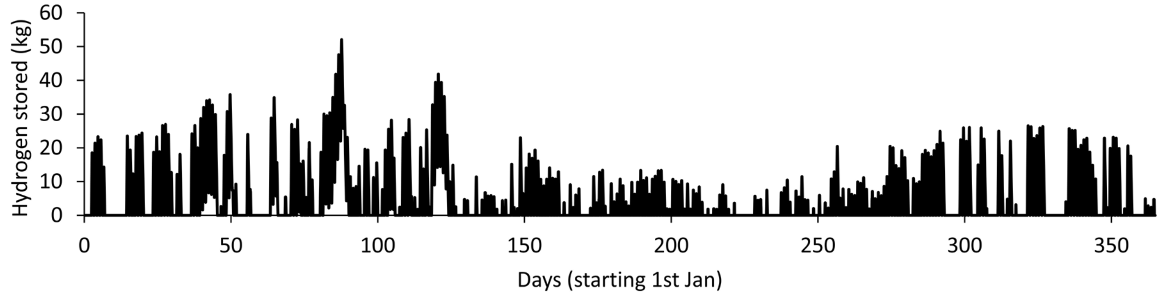

(b)

Figure 7. Annual hourly storage profiles for each case study, with baseline PV capacity and optimally sized rSOC. (a) SE England, (b) Austin, Texas. A long term cycle does emerge for SE England. For Texas, the longest storage cycles are of about a week's duration for this system. Note that cycling is deepest in spring and autumn, when surpluses of solar power are more common.

Table 8. Summary of rSOC impact on microgrid with baseline solar PV capacity and optimised rSOC capacity

	SE England		**Austin, Texas**	
	PV only	**PV + rSOC**	**PV only**	**PV + rSOC**
SSR achieved	0.334	0.423	0.361	0.418
PV per dwelling (kW_p)	3	3	5.52	5.52
rSOC capacity (kW)	0	91.5	0	168.4
Max required H_2 storage (m^3)	0	14.12	0	4.86
Max required H_2 storage (MWh)	0	5.03	0	1.73
Estimated CAPEX	£0.483m	£0.817m	$1.111m	$1.597m
Grid imports (MWh)	255.7	221.6	696.4	634.4
Annual savings	£18466	£23369	$49963	$57838
Payback time (years)	26.2	35.0	22.2	27.6
Payback time versus PV (years)	N.A.	68.1	N.A.	61.7

3.3 Optimisation of installed capacity for each component

Next, the optimiser was permitted to vary the installed capacity of all three components (rSOC, H_2 storage and PV). The intention was to explore scenarios with greater capacity of installed PV, perhaps providing more incentive for long term energy storage. The optimiser searched for the microgrid design achieving lowest CAPEX cost, whilst constrained to achieve a particular SSR. Payback periods were calculated for the microgrid as a whole, relative to a baseline scenario with all power imported from the grid (0% SSR). Results are shown in Figure 8 and Tables 9 and 10.

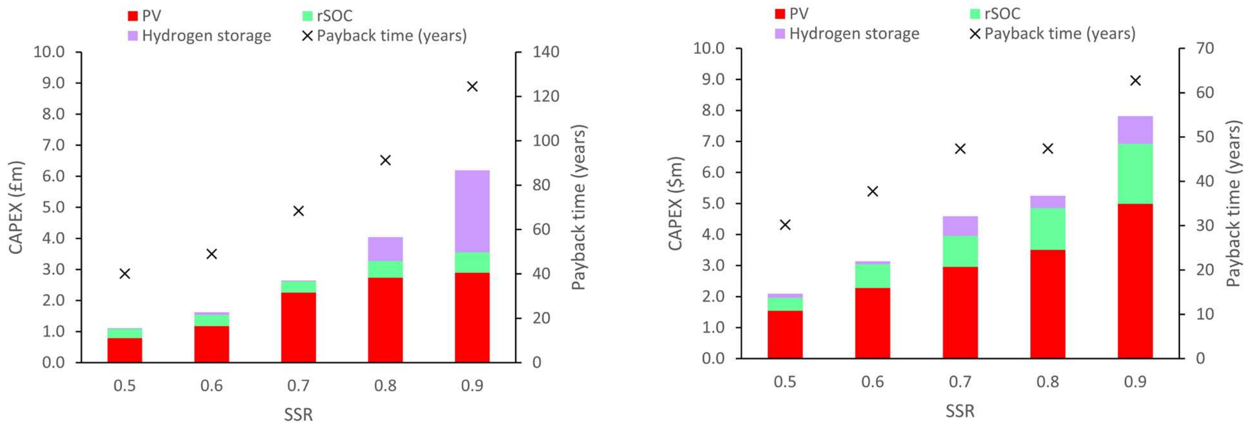

(a) (b)

Figure 8. Estimated CAPEX costs and payback times for systems optimised to achieve specified SSR. (a) SE England, (b) Austin, Texas.

Table 9. Summary of microgrid energy systems for SE England, with CAPEX minimised to achieve given SSR.

SSR requirement	**0.5**	**0.6**	**0.7**	**0.8**	**0.9**
PV per dwelling (kW_p)	4.90	7.30	14.00	16.99	17.98
rSOC capacity (kW)	132.8	149.0	182.0	268.0	329.2
H_2 storage (m^3)	2.1	8.0	2.7	71.6	246.9
H_2 storage (MWh)	0.75	2.85	0.96	25.53	88.03
Estimated CAPEX (£m)	1.077	1.559	2.647	4.037	6.194
Grid imports (MWh)	192.0	153.6	115.2	76.8	38.4
Annual savings (£)	27643	33172	38700	44229	49757
Approx payback time (years)	38.9	47.0	68.4	91.3	124.5

Table 10. Summary of microgrid energy systems for Texas, with CAPEX minimised to achieve given SSR.

SSR requirement	**0.5**	**0.6**	**0.7**	**0.8**	**0.9**
PV per dwelling (kW_p)	7.66	11.32	14.69	17.40	24.80
rSOC capacity (kW)	168.7	305.2	400.0	541.5	773.1
H_2 storage (m^3)	9.6	7.0	47.5	29.5	66.8
H_2 storage (MWh)	3.42	2.50	16.93	10.52	23.82
Estimated CAPEX ($m)	2.090	3.135	4.590	5.250	7.816
Grid imports (MWh)	544.9	435.9	326.9	218.0	109.0
Annual savings ($)	69201	83041	96881	110722	124562
Approx payback time (years)	30.2	37.8	47.4	47.4	62.8

For both case studies, it was possible to design systems achieving SSR of 90% or somewhat above. (100% SSR is not possible without the addition of more flexible, shorter term storage.) In every case, significant capacity of rSOC and H_2 storage was installed by the optimiser (i.e. the required SSR could not be achieved simply by oversizing the PV component). Thus, the rSOC energy storage has value to boost SSR and as such, to boost environmental sustainability.

The high SSR systems would require very large capacities of PV, which is a consequence of the rSOC's low round-trip efficiency. Such large capacities of PV would likely need to be ground-mounted. It will be noticed from Figure 8 that the cost of PV is the most significant part of system CAPEX, until very high SSR is required. For the UK, the H_2 storage volume and cost balloons if SSR above 0.8 is required. For Texas, this does not happen to the same extent, which reflects the reasonable availability of solar power throughout the seasons, as compared to its extreme seasonality in the UK.

Payback periods exceed 30 years in all cases, indicating that the systems would not be financially profitable; furthermore, payback time worsens with increasing SSR. Better payback times are achieved for Texas than for the UK, which may be ascribed to the higher PV capacity factor and better synchronisation of PV and load. Since the energy storage is clearly not financially viable at the high costs and low efficiencies initially assumed, the low cost and high efficiency scenarios are now explored (see Tables 4 and 5 above). As before, the optimiser constrains for SSR and sizes the components to minimise CAPEX. Results are shown in Figure 9 and Tables 11 and 12.

Highly (90%) self-sufficient systems remain too costly in all scenarios. This is especially true for the UK study, with payback times of 80 and 46 years for the two scenarios. Payback periods of < 30 years for the Texas study are more hopeful, although still in excess of the system's likely lifetime. Note that higher efficiency for the energy storage allows for reduction in the required PV capacity, whilst the required rSOC capacity is similar. The impact of increasing rSOC efficiency has more impact in the UK, with the reduced requirement for H_2 storage allowing CAPEX to almost halve.

For systems with modest (50%) self-sufficiency, the economic picture is more interesting. Payback periods of less than twenty years are suggested in both scenarios for Texas, and for the UK if cost and efficiency are both improved. These systems require only a few cubic metres of hydrogen storage, and PV capacities within realistic bounds for rooftop installations. At their present state of maturity, rSOCs cannot be expected to last even for 20 years. SOFCs are capable of running for at least ten years [11], but use in electrolysis mode causes accelerated degradation [4], [5], [29]. Ten years may be a reasonable lifetime for an rSOC stack in the medium term. This suggests that more detailed work is needed, taking the stack replacement cost into account, to establish whether a PV / rSOC / H_2 microgrid can really save versus grid imports over its lifetime.

It may be noted that the impact of increased efficiency is small for the 50% SSR systems; the system becomes 12% cheaper for the UK, and only 2.4% cheaper for Texas. The impact is greatest for the UK 90% SSR system, where the microgrid is 43% cheaper with enhanced efficiency. For the UK, achieving high SSR demands considerable use of storage because of the large seasonal mismatch between load and generation. By contrast, high SSR in Texas is achieved mainly by scaling up solar capacity, with less extra storage capacity needed.

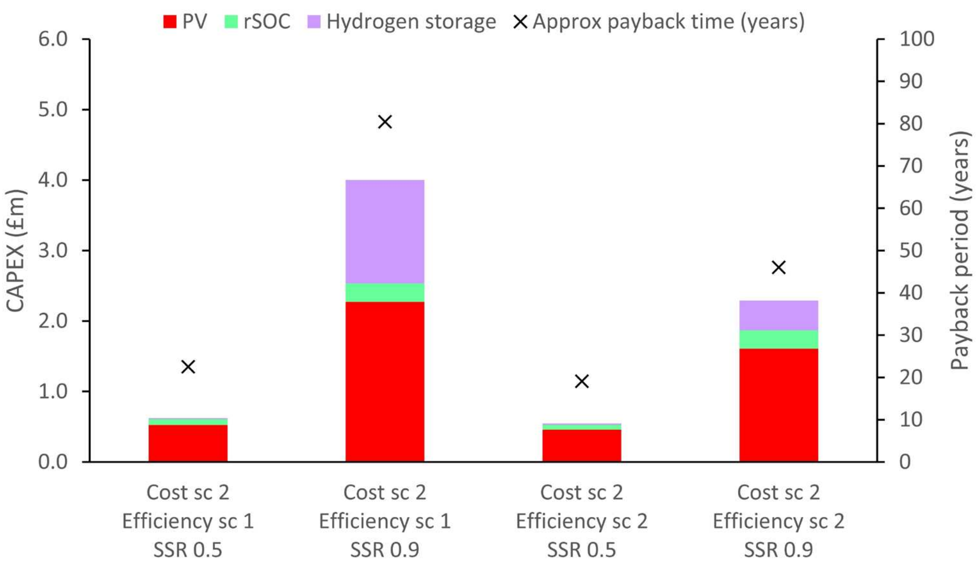

(a)

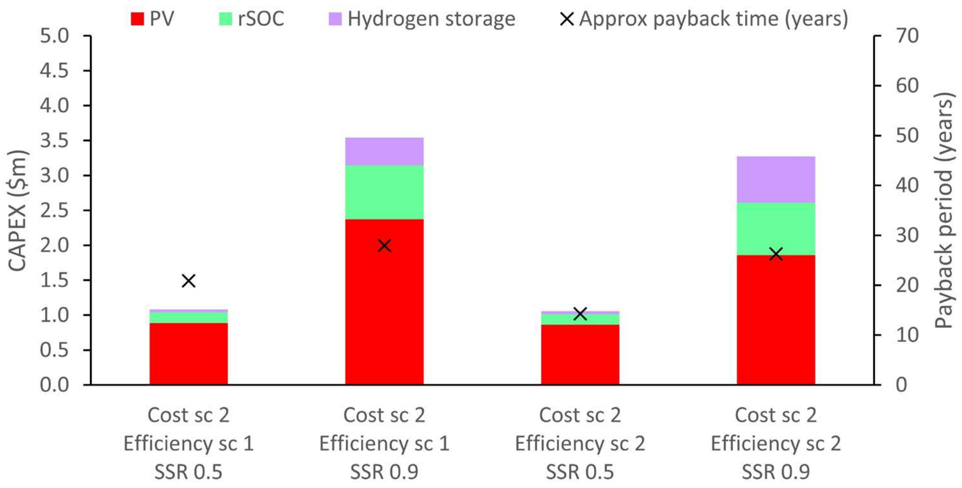

(b)

Figure 9. Estimated CAPEX costs and payback times, under future scenarios. (a) SE England, (b) Austin, Texas.

Table 11. Summary of optimised microgrid energy systems for SE England: future scenarios.

Scenarios	**Efficiency 1, Cost 2**		**Efficiency 2, Cost 2**	
SSR requirement	0.5	0.9	0.5	0.9
PV per dwelling (kW_p)	5.71	24.70	4.99	17.49
rSOC capacity (kW)	110.9	348.0	91.1	346.1
H_2 storage (m^3)	3.9	412.2	5.0	118.3
H_2 storage (MWh)	1.39	146.96	1.78	42.18
Estimated CAPEX (£m)	0.622	4.003	0.545	2.291
Grid imports (MWh)	195.0	39.0	195.0	39.0
Annual savings (£)	27643	49757	27643	49757
Approx. payback time (years)	20.9	80.4	18.4	46.0

Table 12. Summary of optimised microgrid energy systems for Texas: future scenarios.

Scenarios	**Efficiency 1, Cost 2**		**Efficiency 2, Cost 2**	
SSR requirement	0.5	0.9	0.5	0.9
PV per dwelling (kW_p)	7.70	20.63	7.50	16.17
rSOC capacity (kW)	163.9	822.7	160.8	801.4
H_2 storage (m^3)	9.7	89.5	9.7	148.6
H_2 storage (MWh)	3.46	31.91	3.46	52.98
Estimated CAPEX ($m)	1.082	3.542	1.056	3.273
Grid imports (MWh)	544.9	109.0	544.9	109.0
Annual savings ($)	69201	124562	69201	124562
Approx. payback time (years)	15.6	27.9	14.3	26.3

3.4 Results for hybrid energy storage

In this section, results are presented for the SE England study, now with battery storage (BESS) available in addition to rSOC. Similarly to the previous section, four components of the microgrid (PV, BESS, rSOC and H_2 storage) were sized to achieve the specified SSR for minimal payback time. Binary decision variables a_{BESS} and a_{HESS} determined whether BESS and HESS were to be installed. Thus, these results say something about the conditions under which hybrid energy storage (HESS + BESS) is preferable to a system with battery storage only. Scenarios 1 and 2 for efficiency and cost are considered. Details of the optimised microgrid systems are given in Table 13 and in Figures 10-12.

The optimiser exhibited a notable preference to install very large over-capacity of PV, with battery storage, rather than installing HESS. This approach allows for sufficient daily solar generation even during the winter so that the need for long-term bulk energy storage is obviated. Under baseline scenarios for efficiency and cost, even a 90% SSR system is most cheaply achieved without HESS, with 15.25 kW of PV per house. Under the improved scenarios, HESS is not selected until requiring SSR above 85%. It is worth noting that a 90% SSR system using hybrid storage has a payback period of about 37 years; with pure hydrogen based storage the figure was 46 years (see Table 11).

Such large PV installations will not often be feasible in the built environment. Therefore, further results were taken with PV per household constrained below 6 kW. This restriction increases the chance that the HESS is part of the optimal design: the optimiser now selects HESS whenever SSR above 75% is required. This was the case regardless of cost and efficiency scenario. It can be concluded that HESS using rSOC can be an optimal choice when high SSR is desired, whether to achieve high independence from the national grid, or to showcase environmental benefits. These systems are probably not economical, with simple payback period ranging from 20 to 100 years (according to the scenario and the SSR required). Nonetheless, the use of rSOC to obtain the higher SSR and emissions curtailment is implied to be more economical than the use of battery storage alone, if SSR is above the 75% SSR threshold.

Table 13. SE England case study; optimisations with battery / hybrid storage

Scenarios		**Constraints**		**Optimal system design**					**Finances**	
Price Scenario	**Efficiency scenario**	**SSR constraint**	**PV constraint (kW / house)**	**PV (kW / house)**	**BESS (kWh)**	**HESS?**	**rSOC (kW)**	**H_2 storage (m^3)**	**CAPEX (£m)**	**Payback (years)**
1	1	0.9	<20	15.25	1798	No	-	-	3.354	67.2
2	2	0.8	< 20	9.83	1016	No	-	-	1.412	31.9
2	2	0.85	< 20	9.97	651	**Yes**	165.1	42.6	1.518	32.2
2	2	0.9	< 20	13.34	787	**Yes**	138.7	28.7	1.827	36.8
1	1	0.7	< 6	6.00	898	No	-	-	1.415	36.5
1	1	0.75	< 6	6.00	1438	**Yes**	50.0	64.7	2.478	59.6
1	1	0.8	< 6	5.86	1267	**Yes**	56.2	217	4.007	89.6
1	1	0.9	< 6	6.00	2810	**Yes**	169.3	685	10.035	204
2	2	0.6	< 6	4.76	450	No	-	-	0.662	19.8
2	2	0.65	<6	5.40	612	No	-	-	0.803	22.2
2	2	0.7	<6	6.00	929	No	-	-	1.017	26.1
2	2	0.75	<6	5.97	728	**Yes**	64.1	174	1.582	35.6
2	2	0.8	<6	6.00	1106	**Yes**	172.4	202	1.955	42.5
2	2	0.9	< 6	6.00	1815	**Yes**	162.9	331	2.763	54.8

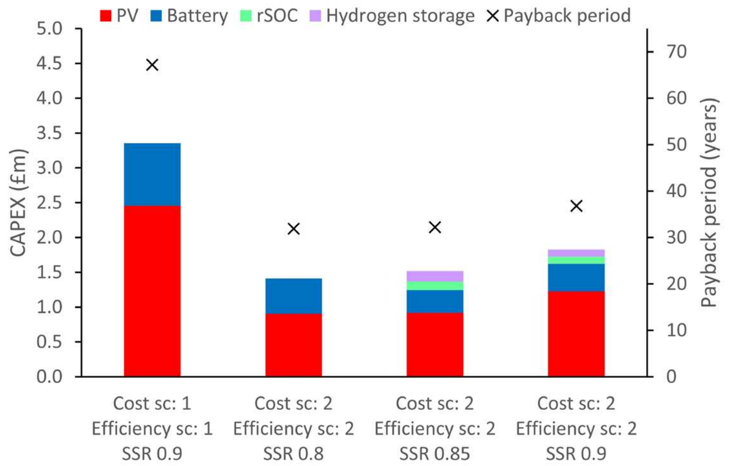

Figure 10. Costs and payback times of optimised microgrid energy systems, with PV capacity constrained below 20 kW.

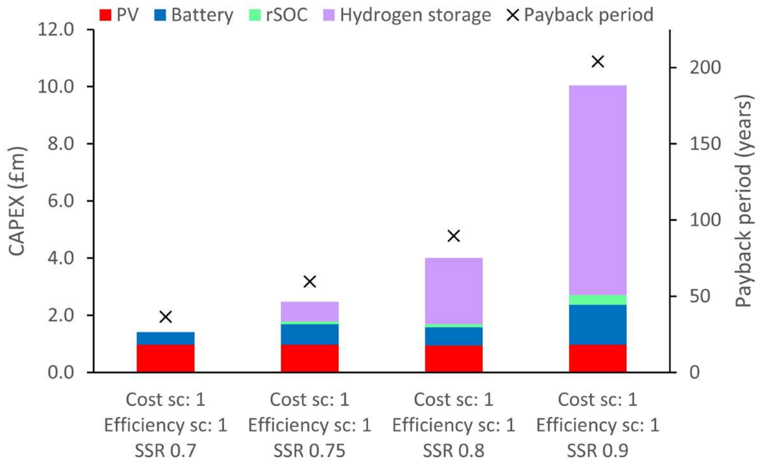

Figure 11. Costs and payback times of optimised microgrid energy systems, with PV capacity constrained below 6 kW. Scenario 1 for cost and efficiency. HESS is selected when SSR above 75% is required.

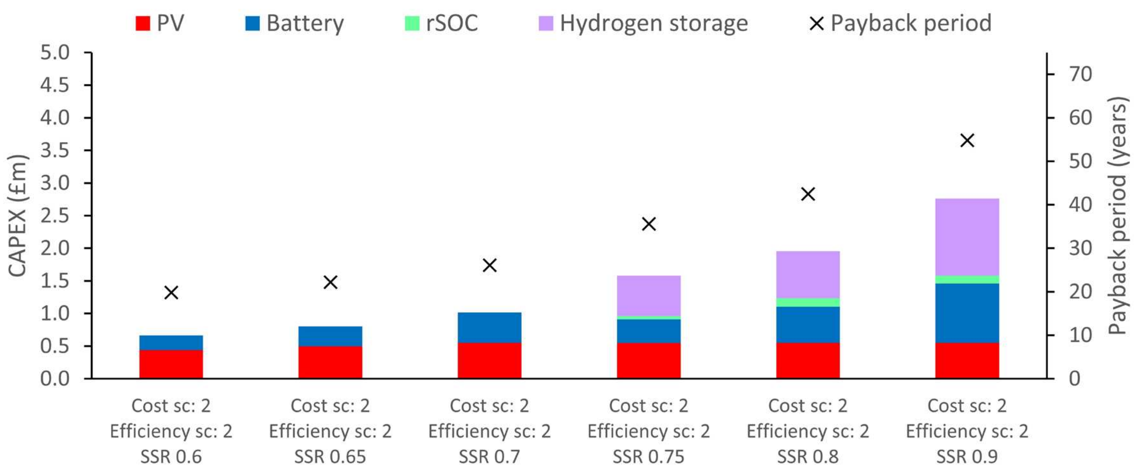

Figure 12. Costs and payback times of optimised microgrid energy systems, with PV capacity constrained below 6 kW. Scenario 2 for cost and efficiency. HESS is selected when SSR above 75% is required.

4. Conclusions and future work

In this paper we have presented an agent-based simulation model for a microgrid equipped with rooftop PV generation, and an rSOC + H_2 storage enabling long term energy storage. This model has been used to quantify the level of grid-independence that such a system could attain, and the consequent cost savings. These benefits have been set against the estimated CAPEX for the microgrid. Two locations have been considered, the south-east of the UK, and Texas, which exhibit differences in both scale and seasonality of solar resource and electricity demand.

Initial simulation work considered households with average-sized PV installations, for each location, and the possible impact of adding the energy storage. In both locations, it was found that the energy storage could allow the microgrid to achieve a self-sufficiency ratio of around 42% over a year, a fairly modest increase from SSR achievable by PV without storage. The cost saving associated with this would not be sufficient to make the energy storage system a viable investment, with payback periods of over six decades indicated. The moderate impact of the storage is partly due to the fact that typical residential PV installations do not generate long-term surpluses of power, in either location. Therefore, subsequent work allowed for PV capacity to be scaled higher.

Next, the capacity of the microgrid's three main components (PV, rSOC, H_2 storage) were optimised in order to achieve given SSR. It was possible to design systems with SSR of 90% or higher. A high SSR is expected to imply similarly high percentage curtailment of the emissions associated with electricity consumption. However, costs increase faster than savings as SSR is increased, with payback times between 30 and 120 years. Systems designed for Texas can be more conservative in scale (relative to the size of annual demand); this is thanks to the solar resource being less seasonal and better synchronised with the load. Consequently, cost-effectiveness is closer to being attainable for Texas. It is also worth noting that the low round-trip efficiency leads to large requirements for PV capacity in order to obtain high SSR.

Two further scenarios were then considered, with lower CAPEX costs and higher rSOC round-trip efficiency. In these scenarios, it was found that a microgrid designed to achieve SSR of 50% could be cost effective over 20 years relative to grid-imported power. Such a design would incorporate hydrogen storage below 10 m^3 volume, providing the equivalent of 10's of kWh of storage per household (about an order of magnitude higher than typical household batteries). Increasing the efficiency of the storage had only a minor effect on system cost for a 50% self-sufficient system; efficiency becomes important if high SSR is required. Accordingly, we conclude that if the lower CAPEX costs shown in Table 4 can be realised, a microgrid designed for 50% self-sufficiency, using rSOC for energy storage, could be cheaper than grid imported power. In addition to reduced costs, rSOC lifetime will need to increase towards (or beyond) the 10-year lifetime currently achievable by SOFCs. (It is worth noting, though, that replacement costs for degraded rSOC stacks would likely only be 20-30% of original CAPEX, since the majority of expense is for balance of plant equipment [77].)

Further work considered the possibilities of using the rSOC in tandem with battery storage for a 'hybrid' energy storage, and the degree to which this can compete with standalone battery storage. It was found that battery storage is in fact preferred to the hybrid storage in many circumstances. However, there is a threshold SSR above which the installation of the rSOC becomes cost-optimal; this threshold appears to be at least 75%, and is higher if the installation of very large capacity PV systems is an option. If it is wished to have a system with SSR above this threshold, to obtain very high environmental benefits and grid independence, the addition of rSOC is advised for the cheapest possible microgrid design. At very high SSR, investment cost and payback period grow very large; financial viability is most plausible for the microgrid with hybrid energy storage with SSR near to the 75% threshold.

The challenging nature of the economics for rSOC energy storage is a common theme in these results, however certain recommendations can be made: firstly, it is notable from Section 3.4 that when HESS is selected, the hydrogen storage component becomes the single most significant cost. It is also known that rSOC efficiency indirectly impacts this (see Figure 9a). Thus, reduction of H_2 storage cost and improvement of rSOC efficiency are priorities. Secondly, payback time may also be improved if the rSOC can realise value in other ways: for instance, by deferring grid upgrades or by supplying heat.

Various directions are suggested for future work:

- Promising microgrid designs should be considered in more detail, with assessment for operating expenditure and equipment replacement costs, as well as possible degradation of equipment.

- The role of mass electric vehicle uptake and its effect on the microgrid's load will be considered.
- The possibility of extracting additional value from the rSOC through utilisation of its waste heat will be considered.
- This work has considered only a flat price for imported electricity, and has not considered the possibility of export tariffs, variable or otherwise. Future work could consider variable import and export tariffs, including under future energy scenarios (where these are expected to fluctuate more dramatically).
- CO_2 abatement has only been considered indirectly via the microgrid's SSR. Future work could quantify CO_2 abatement directly, again with consideration of future scenarios for grid electricity.
- The model should be run at higher time resolution, to allow better study of constraints on rSOC ramp-rate.
- Alternative forms of renewable generation, notably wind, may need to be considered. With less seasonal variation than solar power, the relative advantages of different energy storage technologies may change.
- The agent-based nature of the simulation will be used to study the interaction of individual households with the microgrid and the extent to which they might benefit financially by participating in peer-to-peer energy trading or a bill-sharing scheme.

5. Acknowledgements

Grateful acknowledgement is made of the financial support of the Engineering and Physical Sciences Research Council (EPSRC) in the form of the 'Energy Storage and its Applications' Centre for Doctoral Training under grant code EP/L0168/18; also of the Electric Power Research Institute.

This research makes use of data from the UK Environmental Change Network, UK Power Networks, and Pecan Street Inc.

6. References

[1] F. Zhang, P. Zhao, M. Niu, and J. Maddy, "The survey of key technologies in hydrogen energy storage," *Int. J. Hydrogen Energy*, vol. 41, no. 33, pp. 14535–14552, 2016.

[2] S. B. Walker, U. Mukherjee, M. Fowler, and A. Elkamel, "Benchmarking and selection of Power-to-Gas utilizing electrolytic hydrogen as an energy storage alternative," *Int. J. Hydrogen Energy*, vol. 41, no. 19, pp. 7717–7731, 2016.

[3] J. Auer, J. Keil, and a Stobbe, "State-of-the-art electricity storage systems," *Frankfurt am Main, ...*, p. 16, 2012.

[4] A. Ursúa, L. M. Gandía, and P. Sanchis, "Hydrogen production from water electrolysis: Current status and future trends," *Proc. IEEE*, vol. 100, no. 2, pp. 410–426, 2012.

[5] R. Bhandari, C. A. Trudewind, and P. Zapp, "Life cycle assessment of hydrogen production via electrolysis - A review," *J. Clean. Prod.*, vol. 85, pp. 151–163, 2014.

[6] R. M. Ormerod, "Solid oxide fuel cells," *Chem. Soc. Rev.*, vol. 32, no. 1, pp. 17–28, Dec. 2003.

[7] R. K. Akikur, R. Saidur, H. W. Ping, and K. R. Ullah, "Performance analysis of a co-generation system using solar energy and SOFC technology," *Energy Convers. Manag.*, vol. 79, pp. 415–430, 2014.

[8] M. Lototskyy *et al.*, "A concept of combined cooling, heating and power system utilising solar power and based on reversible solid oxide fuel cell and metal hydrides," *Int. J. Hydrogen Energy*, vol. 43, no. 40, pp. 18650–18663, 2018.

[9] Battelle Memorial Institute, "Manufacturing cost analysis of 1, 5, 10 and 25 kW Fuel Cell Systems for Primary Power and Combined Heat and Power Applications," 2017.

[10] J. Mermelstein and O. Posdziech, "Development and Demonstration of a Novel Reversible SOFC System for Utility and Micro Grid Energy Storage," *Fuel Cells*, vol. 17, no. 4, pp. 562–570, 2017.

[11] "SOFC reaches 11 years in Jülich lifetime test," *Fuel Cells Bull.*, vol. 2019, no. 3, p. 14, 2019.

[12] A. Buttler and H. Spliethoff, "Current status of water electrolysis for energy storage, grid balancing and sector coupling via power-to-gas and power-to-liquids: A review," *Renew. Sustain. Energy Rev.*, vol. 82, no. September 2017, pp. 2440–2454, 2018.

[13] Fuel cells and hydrogen joint undertaking, “Development of water electrolysis in the European Union,” 2014.

[14] Sunfire GmbH, “Steam Electrolysis as the Core Technology for Sector Coupling in the Energy Transition,” 2017. .

[15] M. A. Laguna-Bercero, “Recent advances in high temperature electrolysis using solid oxide fuel cells: A review,” *J. Power Sources*, vol. 203, no. 2, pp. 4–16, Apr. 2012.

[16] K. Chen, S. S. Liu, N. Ai, M. Koyama, and S. P. Jiang, “Why solid oxide cells can be reversibly operated in solid oxide electrolysis cell and fuel cell modes?,” *Phys. Chem. Chem. Phys.*, vol. 17, no. 46, pp. 31308–31315, 2015.

[17] B. Zakeri and S. Syri, “Electrical energy storage systems: A comparative life cycle cost analysis,” *Renew. Sustain. Energy Rev.*, vol. 42, no. 3, pp. 569–596, Feb. 2015.

[18] S. Y. Gómez and D. Hotza, “Current developments in reversible solid oxide fuel cells,” *Renew. Sustain. Energy Rev.*, vol. 61, pp. 155–174, 2016.

[19] V. Venkataraman *et al.*, “Reversible solid oxide systems for energy and chemical applications – Review & perspectives,” *J. Energy Storage*, vol. 24, p. 100782, Aug. 2019.

[20] Sunfire, “About Sunfire,” 2019. [Online]. Available: https://www.sunfire.de/en/company/about-sunfire. [Accessed: 12-Aug-2019].

[21] K. Schwarze, O. Posdziech, J. Mermelstein, and S. Kroop, “Operational Results of an 150/30 kW RSOC System in an Industrial Environment,” *Fuel Cells*, p. fuce.201800194, Apr. 2019.

[22] K. Schwarze, O. Posdziech, S. Kroop, N. Lapeña-Rey, and J. Mermelstein, “Green Industrial Hydrogen via Reversible High-Temperature Electrolysis,” *ECS Trans.*, vol. 78, no. 1, pp. 2943–2952, 2017.

[23] Green Industrial Hydrogen, “GrInHy Project Overview,” 2019. [Online]. Available: https://www.green-industrial-hydrogen.com/. [Accessed: 12-Aug-2019].

[24] O. Posdziech, K. Schwarze, and J. Brabandt, “Efficient hydrogen production for industry and electricity storage via high-temperature electrolysis,” *Int. J. Hydrogen Energy*, vol. 44, no. 35, pp. 19089–19101, Jul. 2019.

[25] S. P. S. Badwal, S. S. Giddey, C. Munnings, A. I. Bhatt, and A. F. Hollenkamp, “Emerging electrochemical energy conversion and storage technologies,” *Front. Chem.*, vol. 2, no. September, pp. 1–28, 2014.

[26] “Jülich scientists report efficiency record for reversible fuel cell,” *Fuel Cells Bull.*, vol. 2019, no. 1, p. 15, Jan. 2019.

[27] Sylfen, “MAJOR TECHNICAL PROGRESS WITH DEMONSTRATOR SMARTHYES,” 2018. [Online]. Available: http://sylfen.com/en/2018/05/22/major-technical-progress-with-demonstrator-smarthyes/. [Accessed: 25-Jul-2019].

[28] P. C. Ghosh, B. Emonts, H. Janßen, J. Mergel, and D. Stolten, “Ten years of operational experience with a hydrogen-based renewable energy supply system,” *Sol. Energy*, vol. 75, no. 6, pp. 469–478, 2003.

[29] I. Dincer and C. Acar, “Review and evaluation of hydrogen production methods for better sustainability,” *Int. J. Hydrogen Energy*, vol. 40, no. 34, pp. 11094–11111, 2014.

[30] Ø. Ulleberg, T. Nakken, and A. Eté, “The wind/hydrogen demonstration system at Utsira in Norway: Evaluation of system performance using operational data and updated hydrogen energy system modeling tools,” *Int. J. Hydrogen Energy*, vol. 35, no. 5, pp. 1841–1852, 2010.

[31] G. Gahleitner, “Hydrogen from renewable electricity: An international review of power-to-gas pilot plants for stationary applications,” *Int. J. Hydrogen Energy*, vol. 38, no. 5, pp. 2039–2061, 2013.

[32] G. Gahleitner, “Hydrogen from renewable electricity: An international review of power-to-gas pilot plants for stationary applications,” *Int. J. Hydrogen Energy*, vol. 38, no. 5, pp. 2039–2061, 2013.

[33] O. Schmidt, A. Gambhir, I. Staffell, A. Hawkes, J. Nelson, and S. Few, “Future cost and performance of

water electrolysis: An expert elicitation study," *Int. J. Hydrogen Energy*, vol. 42, no. 52, pp. 30470–30492, 2017.

[34] Tractebel and Hinicio, "STUDY ON EARLY BUSINESS CASES FOR H2 IN ENERGY STORAGE AND MORE BROADLY POWER TO H2 APPLICATIONS," 2017.

[35] Sylfen, "SYLFEN ANNOUNCES THE FIRST HIGH TEMPERATURE REVERSIBLE ELECTROLYSIS DEMONSTRATOR," 2018. [Online]. Available: http://sylfen.com/en/2018/05/22/press-release-sylfen-announces-the-first-high-temperature-reversible-electrolysis-demonstrator/. [Accessed: 25-Jul-2019].

[36] Sylfen, "THE EUROPEAN PROJECT REFLEX," 2018. [Online]. Available: http://sylfen.com/en/2018/05/22/the-european-project-reflex/. [Accessed: 25-Jul-2019].

[37] V.-T. Giap, S. Kang, and K. Y. Ahn, "HIGH-EFFICIENT reversible solid oxide fuel cell coupled with waste steam for distributed electrical energy storage system," *Renew. Energy*, vol. 144, pp. 129–138, Dec. 2019.

[38] J. Ren, S. R. Gamble, A. J. Roscoe, J. T. S. Irvine, and G. Burt, "Modeling a reversible solid oxide fuel cell as a storage device within ac power networks," *Fuel Cells*, vol. 12, no. 5, pp. 773–786, 2012.

[39] A. Perna, M. Minutillo, and E. Jannelli, "Designing and analyzing an electric energy storage system based on reversible solid oxide cells," *Energy Convers. Manag.*, vol. 159, no. September 2017, pp. 381–395, 2018.

[40] R. K. Akikur, R. Saidur, H. W. Ping, and K. R. Ullah, "Performance analysis of a co-generation system using solar energy and SOFC technology," *Energy Convers. Manag.*, vol. 79, pp. 415–430, 2014.

[41] N. C. Ullvius and M. Rokni, "A study on a polygeneration plant based on solar power and solid oxide cells," *Int. J. Hydrogen Energy*, vol. 44, no. 35, pp. 19206–19223, 2019.

[42] P. Di Giorgio and U. Desideri, "Potential of Reversible Solid Oxide Cells as Electricity Storage System," *Energies*, vol. 9, no. 8, p. 662, Aug. 2016.

[43] C. H. Wendel and R. J. Braun, "Design and techno-economic analysis of high efficiency reversible solid oxide cell systems for distributed energy storage," *Appl. Energy*, vol. 172, pp. 118–131, 2016.

[44] M. Patterson, N. F. Macia, and A. M. Kannan, "Hybrid microgrid model based on solar photovoltaic battery fuel cell system for intermittent load applications," *IEEE Trans. Energy Convers.*, vol. 30, no. 1, pp. 359–366, 2015.

[45] M. J. Khan and M. T. Iqbal, "Pre-feasibility study of stand-alone hybrid energy systems for applications in Newfoundland," *Renew. Energy*, vol. 30, no. 6, pp. 835–854, May 2005.

[46] H. Shahinzadeh, M. Moazzami, S. H. Fathi, and G. B. Gharehpetian, "Optimal sizing and energy management of a grid-connected microgrid using HOMER software," *2016 Smart Grids Conf. SGC 2016*, pp. 13–18, 2017.

[47] A. Maroufmashat *et al.*, "Optimization of renewable powered hydrogen micro-grid; Taking in to account economic criteria," *2016 4th IEEE Int. Conf. Smart Energy Grid Eng. SEGE 2016*, pp. 252–256, 2016.

[48] G. Kyriakarakos, A. I. Dounis, S. Rozakis, K. G. Arvanitis, and G. Papadakis, "Polygeneration microgrids: A viable solution in remote areas for supplying power, potable water and hydrogen as transportation fuel," *Appl. Energy*, vol. 88, no. 12, pp. 4517–4526, 2011.

[49] D. B. Nelson, M. H. Nehrir, and C. Wang, "Unit sizing and cost analysis of stand-alone hybrid wind/PV/fuel cell power generation systems," *Renew. Energy*, vol. 31, no. 10, pp. 1641–1656, 2006.

[50] C. Wang and M. H. Nehrir, "Power management of a stand-alone wind/photovoltaic/fuel cell energy system," *IEEE Trans. Energy Convers.*, vol. 23, no. 3, pp. 957–967, 2008.

[51] P. Gabrielli, M. Gazzani, E. Martelli, and M. Mazzotti, "Optimal design of multi-energy systems with seasonal storage," *Appl. Energy*, vol. 219, no. July 2017, pp. 408–424, 2018.

[52] A. Baldinelli, L. Barelli, and G. Bidini, "Progress in renewable power exploitation: reversible solid

oxide cells-flywheel hybrid storage systems to enhance flexibility in micro-grids management," *J. Energy Storage*, vol. 23, pp. 202–219, Jun. 2019.

[53] M. Sorrentino, A. Adamo, and G. Nappi, "Optimal Sizing of an rSOC-Based Renewable Microgrid," *Energy Procedia*, vol. 159, pp. 237–242, Feb. 2019.

[54] The AnyLogic Company, "AnyLogic," 2019. [Online]. Available: https://www.anylogic.com/. [Accessed: 19-Sep-2019].

[55] J. O. Jensen, Q. Li, and N. J. Bjerrum, "The energy efficiency of onboard hydrogen storage," 2008.

[56] B. Gundogdu, D. T. Gladwin, and D. A. Stone, "Battery SOC Management Strategy for Enhanced Frequency Response and Day-Ahead Energy Scheduling of BESS for Energy Arbitrage," in *IECON 2017 - 43rd Annual Conference of the IEEE Industrial Electronics Society*, 2017.

[57] T. Feehally *et al.*, "Battery energy storage systems for the electricity grid: UK research facilities," *IET Conf. Publ.*, vol. 2016, no. CP684, pp. 1–6, 2016.

[58] Spirit Energy, "Battery Storage Knowledge Bank - Understanding Batteries," *https://www.spiritenergy.co.uk/*, 2020. [Online]. Available: https://www.spiritenergy.co.uk/kb-batteries-understanding-batteries#. [Accessed: 11-Mar-2020].

[59] B. Lawson, "Battery Performance Characteristics," *Electropaedia*, 2005. [Online]. Available: https://www.mpoweruk.com/performance.htm. [Accessed: 11-Mar-2020].

[60] D. Dusabe, J. Munda, and A. Jimoh, "Modelling of cloudless solar radiation for pv module performance analysis," *J. Electr. Eng.*, vol. 60, no. 4, pp. 192–197, 2009.

[61] D. G. Erbs, S. A. Klein, and J. A. Duffie, "Estimation of the diffuse radiation fraction for hourly, daily and monthly-average global radiation," *Sol. Energy*, vol. 28, no. 4, pp. 293–302, 1982.

[62] Sandia National Laboratories, "PVPerformance Modeling Collaborative," 2018. [Online]. Available: https://pvpmc.sandia.gov/modeling-steps/. [Accessed: 10-Jul-2020].

[63] The Green Age, "How many solar panels can I fit on my roof?," 2014. [Online]. Available: https://www.thegreenage.co.uk/how-many-solar-panels-can-i-fit-on-my-roof/. [Accessed: 22-Aug-2019].

[64] UK Environmental Change Network, "UK Environmental Change Network."

[65] PVOutput, "PVOutput," 2020. [Online]. Available: pvoutput.org. [Accessed: 19-Jul-2020].

[66] N. B. Mason, "Solar PV yield and electricity generation in the UK," *IET Renew. Power Gener.*, vol. 10, no. 4, pp. 456–459, 2016.

[67] M. Laguna, "OptQuest: Optimization of Complex Systems," pp. 1–15, 2011.

[68] National Statistics, "Solar photovoltaic (PV) cost data," *gov.uk*, 2019. [Online]. Available: https://www.gov.uk/government/statistics/solar-pv-cost-data. [Accessed: 17-Dec-2019].

[69] E. Rivard, M. Trudeau, and K. Zaghib, "Hydrogen storage for mobility: A review," *Materials (Basel).*, vol. 12, no. 12, 2019.

[70] B. D. James, C. Houchins, J. M. Huya-Kouadio, and D. A. Desantis, "Final Report: Hydrogen Storage System Cost Analysis," no. September, pp. 1–54, 2016.

[71] NREL, "Costs Continue to Decline for Residential and Commercial Photovoltaics in 2018," *nrel.gov*, 2018. [Online]. Available: https://www.nrel.gov/news/program/2018/costs-continue-to-decline-for-residential-and-commercial-photovoltaics-in-2018.html. [Accessed: 15-Apr-2020].

[72] KPMG LLP, "Development of decentralised energy and storage systems in the UK. A report for the Renewable Energy Association," 2016.

[73] OptTek Systems Inc., "OptQuest," 2019. [Online]. Available: https://www.opttek.com/products/optquest/. [Accessed: 20-Aug-2019].

[74] UK Power Networks, "SmartMeter Energy Consumption Data in London Households," 2015. [Online].

Available: https://data.london.gov.uk/dataset/smartmeter-energy-use-data-in-london-households.

[75] National Statistics, “Monthly feed-in tariff commissioned installations,” 2019. [Online]. Available: https://www.gov.uk/government/statistics/monthly-small-scale-renewable-deployment. [Accessed: 20-Jun-2019].

[76] Pecan Street Inc., “Dataport,” 2019. [Online]. Available: https://dataport.cloud/.

[77] R. Scataglini *et al.*, “A Total Cost of Ownership Model for Solid Oxide Fuel Cells in Combined Heat and Power and Power-Only Applications,” no. September, p. 197, 2015.

7. Appendix – details on hybrid storage controller

Table A1. Variables pertaining to the hybrid storage controller.

Symbol	Unit	Definition
$t \in \{0 \ldots 120\}$	-	Hour of forecast period
$d \in \{1 \ldots 5\}$	-	Day of forecast period
$P_{max,d}$	kW	Max AC power to be generated by SOFC during day d
$P_{min,d}$	kW	Max AC power to be consumed by electrolyser during day d
$P_{load,t}$	kW	Forecast electrical load for the microgrid at time t
$P_{gen,t}$	kW	Forecast PV generation for the microgrid at time t
$P_{net,t}$	kW	Forecast net generation for the microgrid at time t (positive sign indicates surplus generation)
$P_{HESS,t}$	kW	Scheduled power for the HESS at time t (positive sign indicates fuel cell mode)
$P_{BESS,t}$	kW	Scheduled power for the BESS at time t. (positive sign indicates discharge)
$P_{imp,t}$	kW	Power imported from grid at time t.
$P_{exp,t}$	kW	Power exported to grid at time t.
$m_{H2,t}$	kg	Mass of hydrogen stored at time t.
m_{full}	kg	Maximum quantity of storable hydrogen
$E_{BESS,t}$	kWh	Energy stored in battery at time t.
C_{BESS}	kWh	Nominal capacity of BESS
η_{comp}	MJ / kg	Energy required for compression of hydrogen
c_{grid}	£ / kWh $ / kWh	Price of grid imported electricity.
c_{store}	£ / kWh $ / kWh	Value assigned to stored energy at the end of the forecast period.

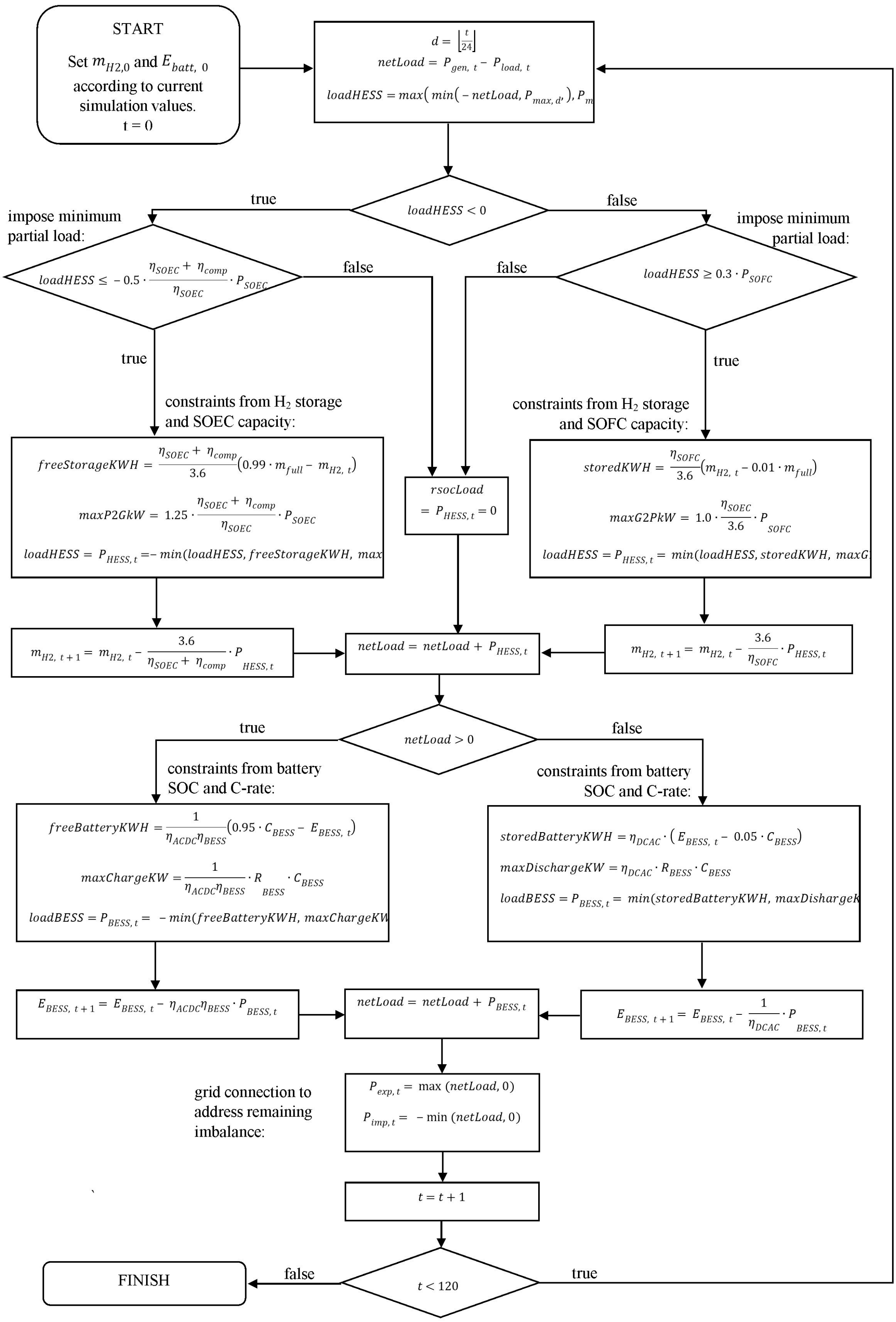

Figure A1. Flowchart showing how a schedule $(P_{HESS,t,}, P_{BESS,t})_{0 \leq t < 120}$ is created for the hybrid energy storage, for given values of $(P_{max,d})_{1 \leq d \leq 5}$ and $(P_{min,d})_{1 \leq d \leq 5}$.